Available online at www.sciencedirect.com
SCIENCE DIRECT
Journal of Crystal Growth 290 (2006) 576–584
JOURNAL OF CRYSTAL GROWTH
www.elsevier.com/locate/jcrysgro

Growth kinetics of CaF_2 in a pH-stat fluidized-bed crystallizer

Clifford Y. Tai[a], P.C. Chen[b,*], T.M. Tsao[a]

[a]Department of Chemical Engineering, National Taiwan University, Taiwan
[b]Department of Chemical and Materials Engineering, Lunghwa University of Science and Technology, Taiwan

Received 1 June 2005; received in revised form 8 February 2006; accepted 15 February 2006
Communicated by M. Uwaha

Abstract

In this study, experiments were first conducted in a stirred vessel to establish the metastable region of calcium fluoride, using a pH-stat apparatus for controlling the pH value of solution. The effects of pH value on the solubility and metastable region were observed. Then, operating variables, including supersaturation, superficial velocity, pH value, seed size, and types of seed and solution, that influenced the crystal growth of the same system were investigated in a fluidized-bed crystallizer. The crystal growth rates were determined from the consumption rates of fluoride ions. The growth kinetics was explored by using the two-step growth model. The effectiveness factor was used to judge whether a controlling step was existing. The kinetics of crystal growth in a lean bed and a dense bed was also discussed.

PACS: 81.10.−h; 81.10 Dn; 81.15 Lm

Keywords: A1. Effectiveness factor; A1. Fluidized bed; A1. Metastable region; A1. Two-step growth model; B1. Calcium fluoride

1. Introduction

Fluorides provide a beneficial effect in preventing dental cavities when an optimum amount of fluoride ion is present in drinking water. However, long-term consumption of drinking water containing excessive amounts of fluoride ion can lead to fluorosis of teeth and bones. On the other hand, fluoride is also a widely used raw material in a number of manufacturing processes, including glass manufacture, electroplating operations, aluminum and steel production, and the manufacture of electronic parts, in which a large quantities of fluoride ion are released in effluents. In some cases, industrial wastewaters containing fluoride ion can be toxic to aquatic organisms, and the presence of fluoride dusts and gases in the atmosphere can be detrimental to plant as well as animal life. Therefore, discharges from these plants must be properly treated and carefully controlled to reduce the degree of contamination to environment.

Although several methods have been applied to remove fluoride ion from aqueous system, such as ion exchange, coagulation, and chemical precipitation, the dewatering cost is high due to the formation of a large amount of sludge. A few papers have been devoted to develop theoretical design models. In many cases, the design of fluoride removal processes is based on empirical equation and past experience. Recently, a pellet reactor, which is a growth-type fluidized-bed crystallizer, has been developed for water softening, fluoride and phosphate removal, and heavy-metals recovery [1]. This clean technology has advantages in the regeneration of material from waste and the reduction in sludge volume in contrast to precipitation process. Thus, the pollution problem is eased and the operation cost is reduced.

The main part of the crystallizer is a cylindrical vessel, partially filled with a suitable seed material, such as filter sand. The inlet stream to the crystallizer, for example, consists of a process effluent of metal-containing wastewater and a circulation stream, to which concentrated carbonate solution is added. The fluid velocity (0.0208–0.0347 m/s) in the crystallizer is high enough to keep the pellets suspending in a fluidized state. The inlet

*Corresponding author. Tel.: +88 62 8209 3211 5205; fax: +88 68 2093211 5201.
E-mail address: chenpc@mail2000.com.tw (P.C. Chen).

0022-0248/$ - see front matter © 2006 Elsevier B.V. All rights reserved.
doi:10.1016/j.jcrysgro.2006.02.036

Nomenclature

A	surface area, m^2/g
a	parameter in Eq. (22)
a_i	activity for species i
b	parameter in Eq. (23)
C	concentration, M
D_a	Damkohler number
f_s	surface shape factor
f_v	volume shape factor
G	linear growth rate, m/s
I	ionic strength, M
IP	ionic product, M^3
K_d	mass-transfer coefficient, m/s
K_{d0}	size-independent mass-transfer coefficient in Eq. (22)
K_i	stability constant for the ith mass action equation
K_r	surface reaction constant, m/s
K_{r0}	size-independent surface reaction constant in Eq. (23)
K_{sp}	solubility product, M^3
L	size of seed crystal, m
M	molecular weight of calcium fluoride, kg/kmol
m	mass of calcium fluoride, kg
Re	Reynolds number
r	reaction order
TCa	total calcium ion, M
TCl	total chloride ion, M
TF	total fluoride ion, M
TNa	total sodium ion, M
t	time, s
u	superficial velocity, m/s
V	volume of solution, m^3
y_z	activity coefficient of z-valent ions, $z = 0,1,2$

Greek letters

ρ_s	density of particle, kg/m^3
σ	relative supersaturation
η	effectiveness factor

stream at the bottom of crystallizer is supersaturated with respect to metal carbonate and this supersaturation acts as the driving force for the crystallization of metal carbonate onto pellets. Metal carbonate deposits and then grows on the surface of pellets. Since the crystal growth should be performed at a lower supersaturation level, an effective control of supersaturation becomes important during an operation. If the generated supersaturation is too high, especially at the bottom of fluidized bed where chemicals mix with the wastewater, it will lead to spontaneous nucleation and mess up the operation. On the other hand, impurity species in solution as well as the pH of the solution influence the solubility of fluoride [2], and hence the supersaturation, which affects the crystal growth rate and the removal rate of pollutant [1,2]. From the viewpoint of thermodynamics, supersaturation is an unstable state. The concentration of solute would sustain at a certain value, which is below the upper limit of metastable region, and the solution would appear stable for a certain period of time. Therefore, the supersaturation of solution must be controlled in the metastable region for the operation of a pellet reactor. Unfortunately, the metastable regions of few sparingly soluble systems were mentioned in the literature.

The concept of metastable regions of sparingly soluble salts was first proposed by Nielsen [3] who expressed the stability chart with the coordinates log[A] and log[B] for electrolyte $A_\alpha B_\beta$. Then the curve corresponding to solubility equilibrium is a straight line, giving a slope of $-\beta/\alpha$, and the supersolubility curve is obtained from experiments. Because the supersolubility curve of CaF_2 is not available at constant pH levels, experiments are required to explore the metastable region.

It is a well-known fact that crystal growth rate depends on supersaturation, temperature, and fluid dynamic conditions. In a pellet reactor, growth rate is also related to the nature of seeds. The selection of proper seeds for crystal growth becomes important in the development of the cleaning process. Besides, the growth rates of sparingly soluble salts are also related to the solution properties, such as ionic strength, pH, and activity ratio [4–7]. Although studies on growth kinetics of sparingly soluble salts were found elsewhere [8–10], most of the experiments were conducted in a stirred tank using seeds below 50 μm with a few cases for the seed size of several-hundred micrometers, which is the suitable size used in a fluidized pellet reactor. For design purpose, a correlation between crystal growth rate of large seeds and process variables of pellet reactor is required.

In this work, experiments were first performed in a pH-stat stirred tank to investigate the metastable region of calcium fluoride. Then, using a pH-stat method, seeded growth experiments were conducted in a fluidized-bed crystallizer with a semi-batch mode to study the effect of process variables on the growth rate of calcium fluoride see Table 1. Two types of seeds, i.e., sand and fluorite, and two types of solutions, i. e., simulated solution and waste solution, were used in this work. The process variables investigated were solution pH, superficial velocity, and seed size. The growth rate data collected in this experiment were analyzed with the two-step growth model with an attempt to explore any controlling step in the growth process, using the effectiveness factor proposed by Garside [11]. Finally, we compared the growth kinetics of CaF_2 in a lean bed and a dense bed of a pellet reactor.

Table 1
Mass action equations [2], total mass balance equations, and activity coefficient equations for $CaCl_2$–NaF–H_2O crystallization system at 25 °C

Mass action equations

$$H_2O = H^+ + OH^-; \quad K_1 = y_1^2[H^+][OH^-] = 1 \times 10^{-14} \tag{1}$$

$$Ca^{2+} + F^- = CaF^+; \quad K_2 = \frac{[CaF^+]}{y_2[Ca^{2+}][F^-]} = 10 \tag{2}$$

$$H^+ + F^- = HF; \quad K_3 = \frac{y_0[HF]}{y_1^2[H^+][F^-]} = 1.5 \times 10^3 \tag{3}$$

$$HF + F^- = HF_2^-; \quad K_4 = \frac{[HF_2^-]}{y_0[HF][F^-]} = 3.9 \tag{4}$$

$$CaOH^+ = Ca^{2+} + OH^-; \quad K_5 = \frac{y_2[Ca^{2+}][OH^-]}{[CaOH^+]} = 10^{-1.327} \tag{5}$$

$$CaF_2(s) = Ca^{2+} + 2F^-; \quad K_{sp} = y_1^2 y_2[Ca^{2+}][F^-]^2 = 10^{-10.31} \tag{6}$$

Total mass balance equations

$$TF = [F^-] + [CaF^+] + [HF] + 2[HF_2^-] \tag{7}$$

$$TCa = [Ca^{2+}] + [CaF^+] + [CaOH^+] \tag{8}$$

$$TCl = [Cl^-] \tag{9}$$

$$TNa = [Na^+] \tag{10}$$

Activity coefficient equations

$$\log y_z = -0.591 z^2 \left(\frac{\sqrt{I}}{1+\sqrt{I}} - 0.2I \right) \tag{11}$$

$$\log y_0 = 0.076I \tag{12}$$

where

$$I = \frac{1}{2} \sum z_i^2 C_i \tag{13}$$

2. Relative supersaturation of calcium fluoride

Relative supersaturation of calcium fluoride solution proposed by Neilsen and Toft [12] is defined as follows:

$$\sigma = (IP/K_{sp})^{1/3} - 1, \tag{14}$$

where IP is the ionic product, defined by $IP = a_{Ca^{2+}} a_{F^-}^2$, and K_{sp} is the solubility product of CaF_2(s). The concentrations of chemical species were calculated from the measured pH, total mass balance equations, and activity coefficient equations (modified Debye–Huckel equation) by successive approximation for the ionic strength [13]. All the equations are also listed in Table 1. Fig. 1 is a plot of relative supersaturation versus pH value for different TCa concentrations, showing that the relative supersaturation increases with an increase in calcium concentration and the pH of solution has no effect on the relative supersaturation when the pH value is higher than 6. The reason is that the chemical species remains constant when the pH value is higher than 6.

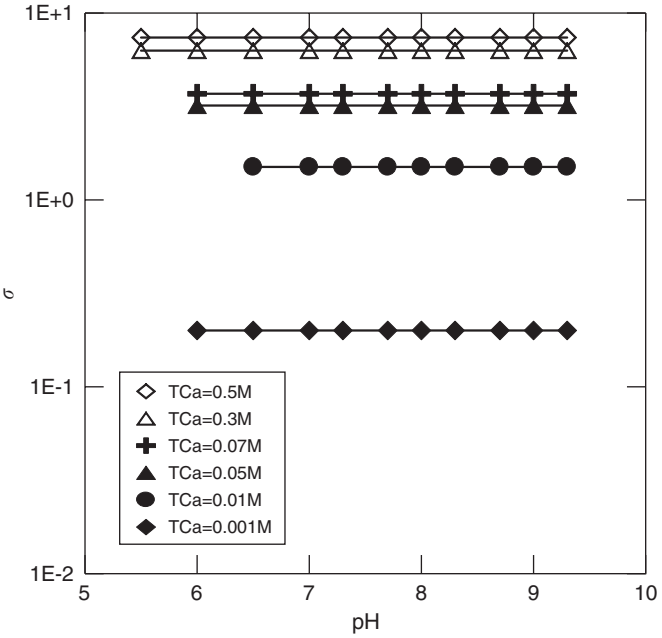

Fig. 1. Relative supersaturation vs. pH at various total calcium-ion concentrations, TF = 0.00057 M.

3. Determination of growth rates

Assuming that the shape factor of crystal remains constant during growth, the linear growth rate is related to mass growth rate by the following expression:

$$G = \frac{dL}{dt} = \frac{f_s}{3 f_v \rho_s A} \frac{dm}{dt}, \tag{15}$$

where m is the mass of calcium fluoride, f_s the surface shape factor, f_v the volume shape factor, ρ_s the density of calcium fluoride and A the surface area. To produce one mole of CaF_2, two moles of fluoride ions are consumed. Therefore, the mass growth rate of calcium fluoride is $d(M[F^-]V/2)/dt$, which is substituted into Eq. (15) to give

$$G = \frac{MV}{6\rho_s} \frac{f_s}{f_v A} \left(-\frac{d[F^-]}{dt} \right). \tag{16}$$

Because the growth rate of calcium fluoride is slow, about 10^{-11} m/s, the surface area available for growth during a run is taken as constant without much error. On the other hand, values of $f_s/f_v A$ for three shapes are constant, which is 1233.84, including cubic, spherical, and cuboid [5]. Therefore, the same value can be applied in this study. Once the total volume of solution consumed, V, the elapsed time, t, and the fluoride ion profile are available, the growth rate of calcium fluoride can be calculated. In this work, the profile of fluoride ion is fitted by a polynomial function:

$$[F^-] = \sum_{i=0}^{N} a_i t^i. \tag{17}$$

Using this equation, the growth rate in Eq. (16) can be obtained at a specified time. For example, the fluoride ion profile of Run no. 1 was

$$[F^-] = 26.0587 - 0.117285t + 3.7443 \times 10^{-4}t^2 - 4.26732 \times 10^{-7}t^3. \quad (18)$$

Substituting Eq. (18) into Eq. (16), the growth rate of calcium fluoride was obtained. The values were 1.55×10^{-10} and 1.24×10^{-10} m/s for the times of 30 and 60 min, respectively. The corresponding supersaturation was calculated from the measured pH, total calcium ion and total fluoride ion, using the method proposed by Nielsen and Toft [12]. The growth rates obtained in this work were in the range from 1.20×10^{-12} to 1.91×10^{-10} m/s, depending on the operating conditions.

4. Growth rate model

A three-step model for the crystal growth was proposed by Kruse and Ulrich [14]. The model takes volume diffusion, surface reaction and heat transfer into account. Generally, the effect of heat transfer did not alter the mass transfer coefficient significantly. Therefore, in order to explore the crystal growth kinetics, the two-step growth model is adopted. The model takes account of the mass-transfer and surface-reaction resistance in series and neglects all other resistance. It is the most used one for crystal growth, since the model is considered suitable for chemical engineering application. At steady-state conditions, the two steps can be represented by the following equations:

$$G = K_d(\sigma - \sigma_i) \quad \text{volume diffusion}, \quad (19)$$

$$= K_r\sigma_i^r \quad \text{surface reaction}, \quad (20)$$

where σ and σ_i are the over-all supersaturation and interfacial supersaturation, respectively. Generally, the interfacial supersaturation is unknown and may be eliminated to give

$$\sigma = \frac{G}{K_d} + \left(\frac{G}{K_r}\right)^{1/r}. \quad (21)$$

If mass-transfer coefficient and surface-reaction coefficient are functions of crystal size,

$$K_d = K_{d0}L^a, \quad (22)$$

and

$$K_r = K_{r0}L^b. \quad (23)$$

Eq. (21) becomes

$$\sigma = \frac{1}{K_{d0}L^a} + \left(\frac{G}{K_{r0}L^b}\right)^{1/r}. \quad (24)$$

When the experimental data of G and σ are obtained, the parameters K_{d0}, K_{r0}, a, b, and r can be estimated by a nonlinear regression method.

Once the parameters are known, the growth mechanism can be explored by using the effectiveness factor proposed by Garside [11]:

$$\eta = (1 - \eta D_a)^r, \quad (25)$$

where D_a is the Damkohler number, which is defined as

$$D_a = \frac{K_{r0}L^{b-a}\sigma^{r-1}}{K_{d0}}. \quad (26)$$

When η approaches zero, the crystal growth is controlled by diffusion. On the other hand, the crystal growth is controlled by surface diffusion for η being 1.

5. Experimental procedure

5.1. Identification of metastable region of calcium fluoride

Because the metastable region of CaF_2 is not available at constant pH levels, experiments are required to establish the supersolubility curve. A simulated solution and a wastewater solution from the semiconductor plant were used to identify the metastable region. First, 100 ml simulated $CaCl_2$ and NaF solutions were mixed together and stirred at 25 °C for at least 2 h, while the pH was kept constant through the action of an autotitrator (AT 200, Kyoto). For a specific concentration of calcium chloride, the solution was clear at low concentration of NaF. Then, the solution became turbid due to nucleation as the concentration of NaF increased further. The boundaries were recorded for various concentrations. From the total calcium ion and total fluoride ion concentrations, a computer program was used to calculate Ca^{2+} and F^- ion concentrations, then to estimate supersaturation. The metastable region of wastewater was obtained in a similar manner. Finally, the metastable region was constructed and all the growth experiments were performed in this region.

5.2. Growth experiments using a fluidized-bed crystallizer

The experimental setup for a semibatch study of crystal growth is shown in Fig. 2, including a fluidized-bed crystallizer and a pH control system (AT 200, Kyoto). The main part of the crystallizer is a PVC column, which is inert to fluoride ion, with 3 cm in diameter and 25 cm in length. Immediately above the column is an enlarged section to prevent seed crystals from carrying over to the reservoir. The pH control system comprises a pH-stat apparatus, a constant temperature bath, and a solution reservoir. Before operation the electrode was standardized with buffers of pH 4 and 7, respectively. Six liters of supersaturated solution of calcium fluoride was prepared by adding simulated solution or wastewater solution into $CaCl_2$ solution already in the reservoir with agitation. Another 0.5 l supersaturated solution was introduced into the crystallizer. Then we started the pump and began the growth experiments. A 3 ml solution was withdrawn from

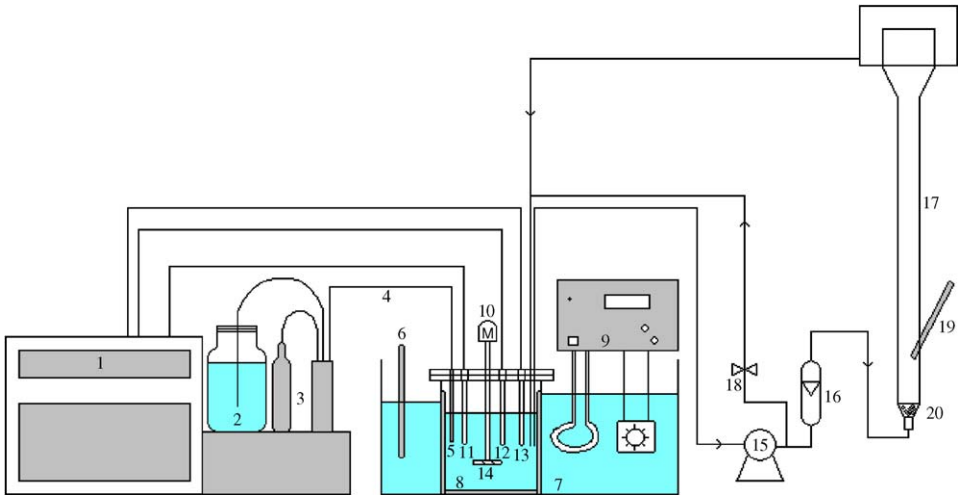

Fig. 2. A pH-stat fluidized-bed crystallization system, 1. pH-controller; 2. Reagent bottle; 3. Pumping system; 4. Feed line; 5. Feed tube; 6. Thermometer; 7. Thermal bath; 8. Storage tank; 9. Heater; 10. Motor; 11. Glass electrode; 12. Reference electrode; 13. Compensation electrode; 14. Stirrer; 15. Pump; 16. Flow meter; 17. Crystallizer; 18. Valve; 19. Thermometer; 20. Distributor

Table 2
Operating conditions of fluidized-bed experiments conducted in this work

Working temperature (°C)	25
Superficial velocity (m/s)	0.0236–0.0519
pH range	8.0–10
Relative supersaturation	1.0–2.5
Seed size (μm)	
Fluorite	250–600
Sand	300–600
Weight of seeds (g)	10–40

Table 3
The composition of simulated solution and waste water used in this work

Composition	Simulated solution (M)	Waste water (M)
F^-	0.001–0.1	2.83
Al^{3+}	—	1.41×10^{-5}
Fe^{3+}	—	5.01×10^{-5}
Si^{4+}	—	0.023
Ca^{2+}	0.00005–0.1	1.15×10^{-4}
Mg^{2+}	—	3.62×10^{-5}
Na^+	0.001–0.1	1.96×10^{-3}
Zn^+	—	6.18×10^{-5}

the crystallizer by a syringe every 30 min and filtered with a 0.22 μm filter. Subsequently, the fluoride ion was determined by an ion-meter and the crystal growth rate was estimated by the consumption rate of fluoride ion. The operating conditions are listed in Table 2.

6. Results and discussion

6.1. Metastable region of calcium fluoride

The metastable region of calcium fluoride was studied in a stirred tank for a simulated solution and a waste stream from a semiconductor plant. The solution compositions of both systems are shown in Table 3. From the concentration data obtained at the boundary between turbid and clear state, a plot of pCa^{2+} versus pF^- is shown in Fig. 3. The solubility curve (dotted line) and supersolubility curve (solid line) divided the diagram into three areas for the two different solutions. Three areas are undersaturated region, metastable region and labile region, respectively. The metastable region is wider for the wastewater, because the compositions of the two solutions are quite different. The effect of impurity on the nucleation rate was observed

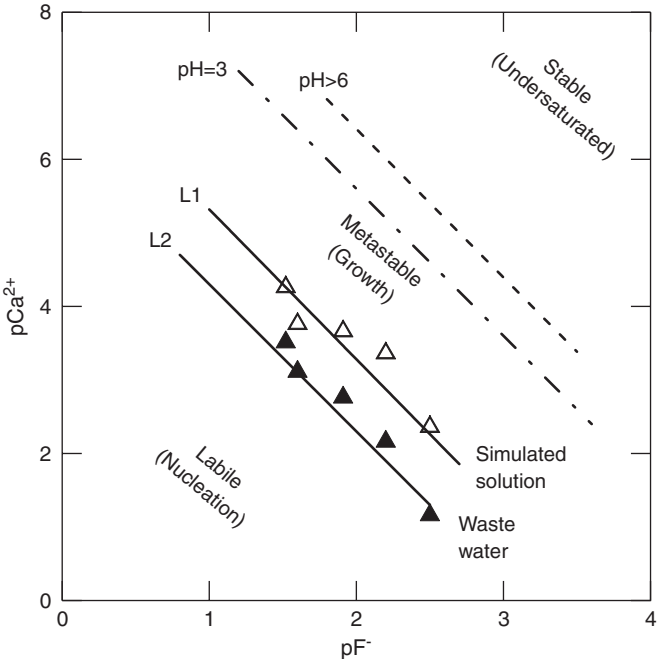

Fig. 3. Metastable regions of calcium fluoride for waste water from a semiconductor plant and a simulated solution at pH = 8.

by Sellami et al. [15] in a precipitation experiment of $CaCO_3$. In addition, the supersolubility curves, i.e., L1 and L2 for simulated and waste systems are close to a straight line with a slope of -2 for both systems. These two lines are almost parallel to the solubility curve of an electrolyte $A_\alpha B_\beta$ with $\beta/\alpha = -2$ [3]. However, the result is slightly different from that reported by Tai [7] for calcium carbonate system, which has curved lines. This is because the ion pairs, complex ions and pH of the solution had a more strong effect on the calcium carbonate system. In addition, the metastable regions found for both solutions can be used at a pH value which is higher than 6.

6.2. Effects of ionic strength and activity ratio

In this work, the effect of ionic strength on the growth rate was not significant unless the ionic strength was higher than 0.5 M [5]. In the literature, Kralj and Brecevic [16] found that ionic strength has a slight effect on the growth rate of vaterite in the range from 0.015 to 0.115 M; the growth rate at high ionic strength was about 15% higher than that at low ionic strength. The effect of ionic strength on the growth of calcite in the ionic strength ranging from 0.0025 to 0.034 M was found by Tai [7]. The effect of ionic strength can be explained as follows. For CaF_2 at low ionic strength, say, 10^{-3} M, the activity coefficient, y_2, is 0.98, which is close to the activity of an ideal solution. In addition, the double-layer thickness does not change at such a dilute solution. For example, for the ionic strength of 0.001 and 0.005 M, the thickness is 6.26 and 3.98 nm, respectively, while at ionic strength of 0.5 M the thickness is 0.4 nm, which is highly compressed at this high ionic strength. The ionic strength appears to influence the growth rate, since the adsorption of growth unit on the crystal surface was easier under such a small thickness of double layer. It is concluded that the higher the ionic strength, the greater the growth rate [16,17]. On the other hand, it was found that the growth rates for $Ca/F > 1$ and $Ca/F < 1$ showed different growth kinetics; the growth rate for $Ca/F > 1$ was always higher than that for $Ca/F < 1$. Further studies on other process variables, including supersaturation, crystal size, pH, and superficial velocity, the ionic strength and activity ratio were kept below 0.01 M and 1, respectively, in order to reduce the errors caused by the variation of these two variables.

6.3. Effect of superficial velocity

The relative velocity, which increases with an increase in superficial velocity, between particle and solution influences the crystal growth rate. Experiments were conducted for different superficial velocities, namely, 0.0236, 0.0331, 0.0425, and 0.0519 m/s, at pH 8 in the crystallizer loaded with an appropriate amount of 388 μm fluorite seed, from 10 to 40 g depending on the superficial velocity. The results are shown in Fig. 4. Under the same supersaturation, the crystal growth rates are greater for higher superficial velocities; the difference is significant with an increase to about five times for the velocity changing from 0.0236 to 0.0519 m/s. However, a high velocity is not always advantageous in an operation, since the bed expands more at high superficial velocities. Increasing superficial velocity from 0.0331 to 0.0425 m/s, the expansion ratio is 3.7 for the former and 12.3 for the latter. A high expansion ratio means a small loading of the crystallizer, and thus a smaller surface area available for crystal growth. As a result, there exists an optimum superficial velocity. In practice, superficial velocity is set between 0.0139 and 0.033 m/s [18].

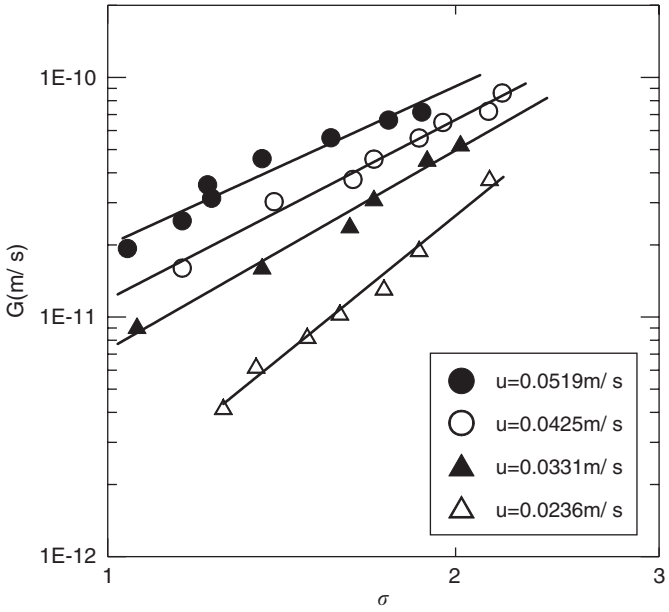

Fig. 4. Growth rate of calcium fluoride vs. relative supersaturation at various superficial velocities, using a seed size of 388 μm.

6.4. Effects of pH value on growth rate in a lean and a dense bed

The pH value has no effect on the supersaturation of solution, as shown in Fig. 1. However, it has a tremendous effect on the crystal growth rate. The results are shown in Fig. 5 for both lean bed ($u = 0.0519$ m/s) and dense bed ($u = 0.0236$ m/s). In the same figure it also indicates that the higher the pH value, the greater the growth rate for both beds. An increase of 2-fold in growth rate for an increase in pH value of 1. Thus, the throughput of a pellet reactor is higher at higher pH values. However, maintaining at high pH value, the consumption of alkali solution will increase, which means higher operation cost. At higher pH values, solute in solution accelerates to deposit on the crystal surface, and hence the growth rate. The marked dependence of growth rate on pH value is probably due to the change of electric charge on crystal surface [19]. The dependence of growth rate on the pH value was found for other systems, such as potassium chloride [6] and lead fluoride [17,20].

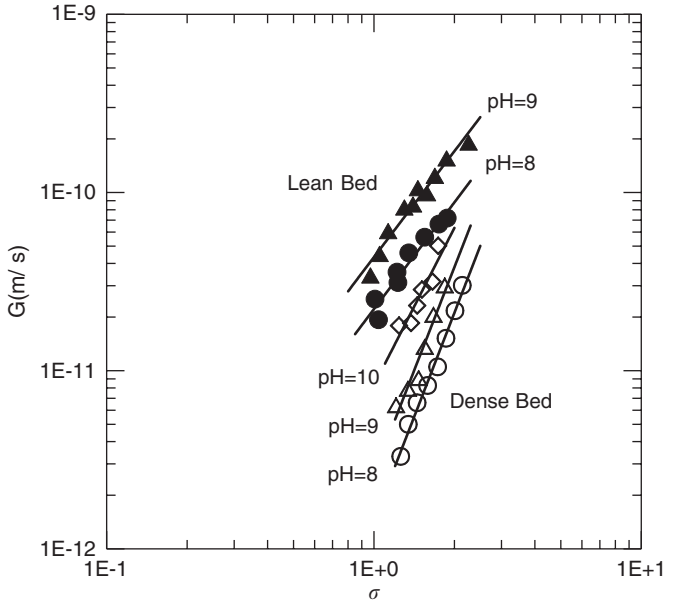

Fig. 5. Comparison of growth rates of calcium fluoride for a lean bed and a dense bed, using a seed size of 388 μm.

6.5. Effects of seed size and type

In order to investigate the effects of seed size and type in the two different solutions experimental results were collected for three groups as shown in Fig. 6, in which Group I is for the simulated solution seeded with fluorite; Group II is for the simulated solution seeded with sand; and Group III is for the waste water from a semiconductor plant seeded with fluorite. For the three groups, the results show that crystal growth rates increase with an increase in crystal size. It may be caused by growth dispersion as recognized by crystallization community [21].

In the simulated solution the growth rate of sand is about one-third of fluorite. The difference is probably due to the difference in surface structure although the sand was fully covered with calcium fluoride. Using fluorite as seed, the growth rates in the waste solution are higher than those in the simulated solution. It is conjectured that some impurities existing in the waste stream augment the growth rate; however, the identification of active species is difficult.

6.6. Crystal growth rate expression

According to the two-step growth model, the crystal growth rate expressions of different seed types and of different fluoride-ion sources are shown in Table 4. The regression errors, according to the definition proposed by Gerald [22], for GI, GII, and GIII are 0.278, 0.266, and 0.194, respectively. It is worth noting that there is a difference in the kinetic order of surface reaction between sand and fluorite, about 2 for the former and 3 for the latter. This result is not surprising because we expect the surface structures of the two seeds are different. The result

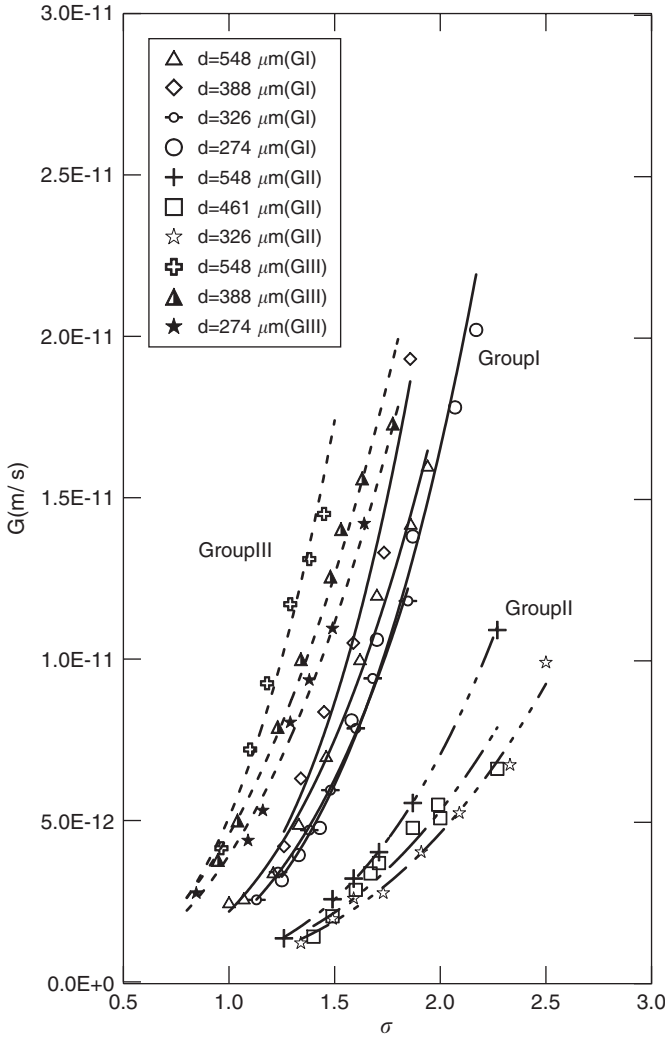

Fig. 6. Comparison of growth rates of calcium fluoride for two types of seed, sand and fluorite (GI and GII), as well as for two types of solution, waste water from a semiconductor plant and a simulated solution (GI and GIII), $u = 0.0236$ m/s.

indicates that the growth rates are not significantly influenced by seed size. In the size range studied (250–600 μm), the growth rate varied at most by 20% as calculated from $(600/250)^{0.21}$, where 0.21 is the exponent of L for the Group III. When we compare the kinetic expression of Group I with Group III, we found that the exponent on supersaturation did not change much. It means that the impurities in the waste solution do not change the value of r. This is similar to the experimental results for the effect of dye on the growth rate of magnesium sulfate [23], but contrary to those for the effect of $CrCl_3$ on the growth rate of magnesium sulfate. A possible reason has been proposed by Tai et al. [24] using the BCF theory. On the other hand, the effect of seed size means that the effect of setting velocity together with growth rate dispersion gives so nicely correlated as size-dependent growth. As far as the crystal growth mechanism is concerned, the effectiveness factor is plotted against

Table 4
Kinetic expressions for different crystallization systems

Seed type	Size range (μm)	Type of solution	Kinetic expression	Error
Fluorite (GI)	250–600	Simulated solution	$G = 4.26 \times 10^{-12} L^{0.20}(\sigma - \sigma_i)$ $= 3.28 \times 10^{-12} L^{0.19} \sigma_i^{3.16}$ (27)	0.278
Sand (GII)	300–600	Simulated solution	$G = 8.80 \times 10^{-12} L^{0.03}(\sigma - \sigma_i)$ $= 7.39 \times 10^{-13} L^{0.18} \sigma_i^{1.92}$ (28)	0.266
Fluorite (GIII)	250–600	Waste water	$G = 5.20 \times 10^{-12} L^{0.21}(\sigma - \sigma_i)$ $= 4.75 \times 10^{-12} L^{0.19} \sigma_i^{3.06}$ (29)	0.194

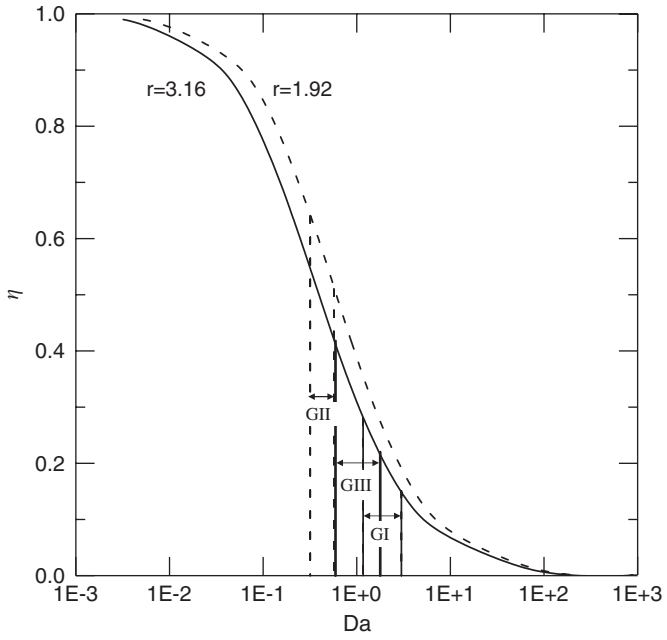

Fig. 7. A plot of η vs. D_a for GI, GII, and GIII with seed size in the range between 250 and 600 μm. Crystallizer was operated at pH = 8 and $u = 0.0236$ m/s.

Damkohler number as shown in Fig. 7. It should be noted that the η–D_a curves for $r = 3.16$ and 3.06 coincide. The D_a ranges found for the three groups indicate that mass-transfer and surface-reaction resistances are significant and there is no controlling step.

7. Conclusion

The metastable regions of calcium fluoride in simulated solution and waste solution were found in a pH-stat stirred tank. The experimental data showed that solubility and supersolubility curves tend to be parallel by plotting pCa^{2+} vs. pF^-. In the metastable region, the growth rate of calcium fluoride crystals measured in a fluidized bed increases with an increase in supersaturation, pH value, superficial velocity, and seed size. However, the effect of ionic strength on growth rate is less significant. The growth rate changes with the types of seed and solution, and is less influenced by crystal size for either sand or fluorite seeds. The different growth rates of various crystal sizes indicated that the growth rate increases with seed size. For the operation conditions used in this experiment, both mass-transfer and surface-reaction resistances are important in the growth process as judged from the effectiveness factor.

References

[1] J.C. Van Dijk, D.A. Wilms, J. Water SRT-Aqua 40 (5) (1991) 263.
[2] J.N. Butler, Ionic Equilibrium, Addison-Wesley, Reading, MA, 1964, p. 284.
[3] A.E. Nielsen, J. Crystal Growth 67 (1984) 289.
[4] C.Y. Tai, C.H. Lu, C.K. Wu, J. Chin. Inst. Chem. Engs. 36 (2005) 443.
[5] T.M. Tsao, Crystal Growth Kinetics of Calcium Fluoride, Master Thesis, National Taiwan University, Taiwan, 1995.
[6] S. Sayed, G. Sultan, W. Omar, H. Mohameed, J. Ulrich, in: Proceedings of Industrial Crystallization, vol. 1, 1996 p. 147.
[7] C.Y. Tai, J. Crystal Growth 206 (1999) 109.
[8] P.C. Tseng, G.T. Rochelle, Environ. Prog. 5 (1986) 5.
[9] J. Christoffersen, M.R. Christoffersen, J. Crystal Growth 100 (1990) 203.
[10] C.Y. Tai, P.C. Chen, S.M. Shih, AIChE J 39 (9) (1993) 1472.
[11] J. Garside, Chem. Eng. Sci. 26 (1971) 1425.
[12] A.E. Nielsen, J.M. Toft, J. Crystal Growth 67 (1984) 278.
[13] G. Nancollas, Interactions in Electrolyte Solutions, Elsevier, London, 1966, p. 80.
[14] M. Kruse, J. Ulrich, A Three-Step Model of Crystal Growth Incorporating Mass and Heat Transfer Phenomena, in: proceedings of the 12th Symposium on Industrial Crystallization, vol. 2, 1993, pp. 4-125.
[15] J. Sellami, N. Frikha, M.E. Plasari, Simultaneous Nucleation Rate Determination of Calcite and Aragonite in the Presence of Citrate Ions, Industrial Crystallization, 2002 (CD-ROM).
[16] D. Kralj, L. Brecevic, J. Crystal Growth 104 (1990) 793.
[17] N. Stubicar, B. Markovic, A. Tonejc, M. Stubicar, J. Crystal Growth 130 (1993) 300.
[18] C. Dotremont, D. Wilms, D. Devogeleare, A. Van Haute, J. Van Dijk, in: L. Pawlowski, et al. (Eds.), Chemistry for Protection of the Environment, Plenum Press, New York, 1991, p. 741.
[19] T.G. Foxall, C. Peterson, H.M. Rendall, A.L. Smith, J. Chem. Soc. Faraday Trans. 75 (1979) 1034.
[20] N. Stubicar, M. Scrbak, M. Stubicar, J. Crystal Growth 100 (1990) 261.

[21] A.H. Janse, E.J. de Jong, Ind. Cryst. 78 (1979) 135.
[22] C. F. Gerald, Applied Numerical Analysis, First ed., Addison-Wesley, Reading, MA, 1978, p. 473 (Chapter 10)
[23] C.Y. Tai, C.H. Lin, J. Crystal Growth 82 (1987) 377.
[24] C.Y. Tai, C.S. Cheng, Y.C. Huang, J. Crystal Growth 123 (1992) 236.